ENSO-Driven Modulation of the Caribbean Subsurface Salinity Maximum

Yongfei Deng[1], Tianning Wu[1], Joseph C. Gradone[2], W. Douglas Wilson[3], Travis N. Miles[2], and Ruoying He[1,*]

[1]Department of Marine, Earth, and Atmospheric Sciences, North Carolina State University, Raleigh, North Carolina, USA

[2]Department of Marine and Coastal Sciences, Rutgers University, New Brunswick, New Jersey, USA

[3]Center for Marine and Environmental Studies, University of the Virgin Islands, St. Thomas, U.S. Virgin Islands, USA

[*]Corresponding author: rhe@ncsu.edu

Abstract

This study identifies El Niño–Southern Oscillation (ENSO) as the primary driver of interannual subsurface salinity variability in the Caribbean Sea. Using 30 years of high-resolution, data-assimilative ocean reanalysis (1993–2022), we show that the Subsurface Salinity Maximum (SSM) closely tracks ENSO cycles: El Niño events correspond to a saltier and deeper SSM, while La Niña drives a fresher and shallower SSM, with contrasts of ~+0.028 to +0.054 g kg^{-1} in salinity and ~+10 m in depth. Two coupled mechanisms govern these shifts: local wind stress curl anomalies inducing anomalous Ekman downwelling or upwelling, driving vertical SSM displacements; and enhanced or reduced remote advection of Subtropical Underwater (STUW) from the North Atlantic Subtropical Gyre, delivering anomalous salinity into the SSM layer. These findings position the Caribbean as a critical node where Pacific climate signals are imprinted onto Atlantic hydrography, with implications for upper-ocean buoyancy and North Atlantic circulation and climate predictability.

Introduction

The Caribbean Sea plays a crucial role in the Atlantic Ocean circulation, acting as a conduit between tropical and subtropical water masses and a key component of the upper limb of the Atlantic Meridional Overturning Circulation (AMOC)[1–3]. Through its western boundary connection to the Yucatan Channel and the Loop Current system in the Gulf of Mexico, the Caribbean regulates the export of warm, saline waters toward the North Atlantic[4]. Variability in Caribbean water properties therefore has implications that extend beyond the regional scale, potentially influencing North Atlantic climate feedbacks and global thermohaline circulation[5].

Among the key hydrographic features in the Caribbean Sea is the presence of a subsurface salinity maximum (SSM) layer, typically centered between ~100–190 m depth[6, 7]. This layer is primarily associated with the Subtropical Underwater (STUW), a water mass formed in the North Atlantic Subtropical Gyre[6] through excess evaporation over precipitation and thus characterized by high salinity. The saline STUW is advected westward by the North Equatorial Current and enters the Caribbean mainly through the Leeward Island and Windward Island Passages (Fig. 1a). The properties of this water mass, particularly its salinity maxima, significantly influence upper-ocean stability and heat content; consequently, they serve as sensitive indicators of surface forcing and ocean–atmosphere coupling within the subtropical gyre[5, 8, 9].

While the climatological structure of the Caribbean Sea and its connection to the western boundary circulation have been well studied, less is known about the interannual to decadal variability of its water mass properties[5], and how this variability links to large-scale climate modes. Previous studies have shown that ENSO (El Niño–Southern Oscillation), the largest signal in interannual climate variation[10], strongly modulates the atmospheric and oceanic circulation over the tropical Atlantic and Caribbean region, altering sea level pressure[11], wind stress[12], sea surface height and surface circulation[13], and mean current and eddies[14]. However, the mechanisms through which ENSO influences subsurface salinity variability in the Caribbean Sea, particularly the SSM layer, remain poorly quantified.

This study aims to fill that gap by investigating the ENSO-driven modulation of the maximum salinity water in the Caribbean Sea. Using a high-resolution, data-assimilative ocean model spanning 1993–2022, we quantify how ENSO alters local and remote forcing mechanisms, including wind stress curl associated with large-scale atmospheric circulation and the advection of STUW, to drive interannual variability in the SSM layer.

Specifically, we address the following questions:

1. What is the spatial and temporal variability of the Caribbean Sea's SSM and its associated depth on interannual timescales?

2. How does ENSO modulate this variability through large-scale wind and ocean circulation anomalies?

3. What are the relative roles of local forcing (e.g., wind stress) and remote processes (e.g., STUW advection, subtropical gyre changes)?

By elucidating these connections, this study provides new insight into how tropical–subtropical coupling regulates the physical state of the Caribbean Sea and its potential response to long-term climate variability.

Results

Climatological structure and variability

The Caribbean Sea contains a well-defined SSM associated with Subtropical Underwater (STUW), centered between 100–190 m (Fig. 1d). The mean salinity maximum ($S_{\max} > 36.5$ g kg^{-1}) occurs in most parts of the Caribbean and weakens westward as the water mass mixes along its pathway toward the Yucatan Channel (Fig. 1c; Supplementary Fig. 1). The depth of the salinity maximum ($Z_{\max S}$) deepens from about 50 m in the southeast to 200 m in the northwest (Fig. 1d), following the southeast–northwest mean circulation characterized by the Caribbean Through-flow (CTF; Fig. 1b).

The 2–7 year bandpass-filtered standard deviations of $S_{\max}$ and $Z_{\max S}$ anomalies show that the interannual variability of $S_{\max}$ reaches 0.05 g kg^{-1} (Fig. 1e), strongest in the eastern Caribbean where mesoscale eddy activity and wind forcing variability are pronounced[15]. The spatial distribution of associated vertical displacements of $Z_{\max S}$ (up to ±10 m) aligns closely with the mean flow patterns, suggesting that dynamic height and wind forcing may play major roles in modulating the vertical structure of this subsurface salinity core (Fig. 1f).

ENSO-related forcing and oceanic response

ENSO exerts a dominant influence on the Caribbean through atmospheric teleconnections that alter regional wind stress and atmospheric circulation patterns (Fig. 2). During El Niño, strengthened easterlies and negative wind stress curl anomalies dominate the Caribbean, which may contribute to enhanced inflow of CTF and Ekman pumping, and ultimately increase the SSM and deepen the halocline (Fig. 2b).

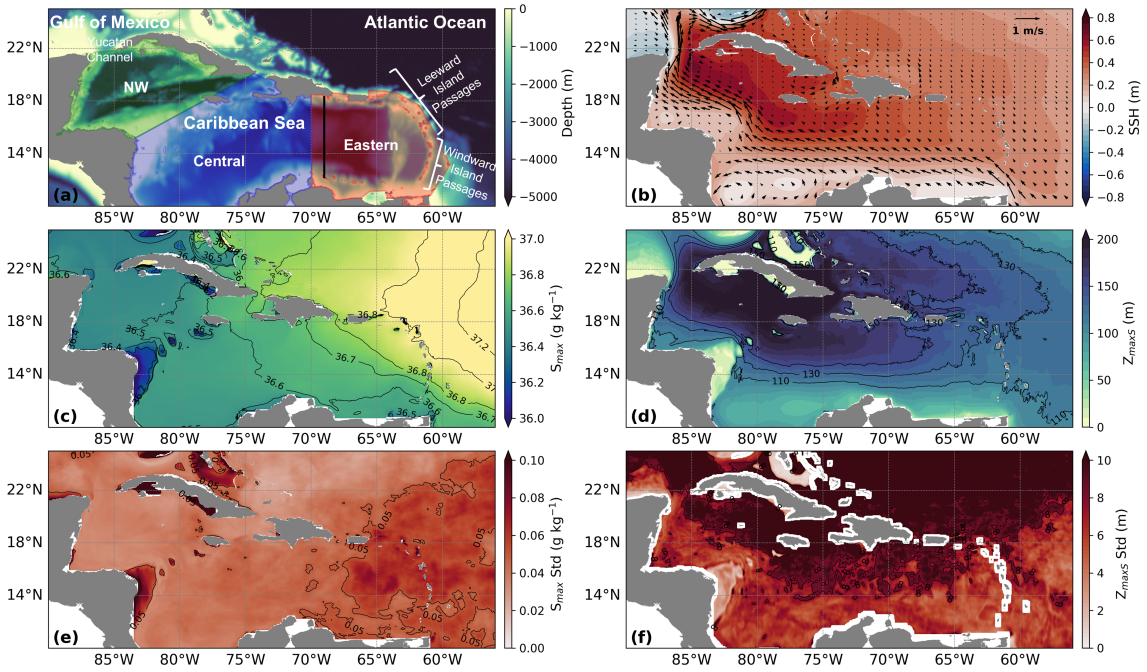

Fig. 1. Climatology and interannual variability of the Caribbean Subsurface Salinity Maximum. (**a**) Topography and subdomains of the Caribbean. (**b**) Mean circulation and sea surface height. (**c**,**d**) Climatological maximum salinity ($S_{\max}$) and its associated depth ($Z_{\max S}$). (**e**,**f**) Standard deviations of 2–7 year bandpass-filtered monthly $S_{\max}$ and $Z_{\max S}$. In (**f**), the pattern is smoothed using a 2D Gaussian filter.

Conversely, La Niña weakens easterlies and CTF, generates positive wind stress curl (WSC) anomalies, enhances Ekman suction, and shoals the halocline.

Correlation analyses between ONI (Fig. 2a) and model-derived salinity fields reveal a coherent response across the basin (Fig. 2c,d). $S_{\max}$ is positively correlated with ONI over the whole Caribbean except in the vicinity of the south part of the Windward Islands where the Amazon freshwater plume concentrates and flows through[16–18] (Fig. 2c). $Z_{\max S}$ and ONI are also positively correlated across the Caribbean (Fig. 2d), indicating that El Niño events are associated with a saltier, deeper SSM and La Niña with a fresher, shallower layer in most parts of the Caribbean.

The vertical structure of salinity shows that significant interannual variations associated with ENSO events take place in the water column across the entire Caribbean. A salinification trend over the 1993–2022 period in the subsurface layer is seen in all subdomains: NW, Central, and Eastern Caribbean (Fig. 3a–c, see also Supplementary Fig. 1), consistent with independent Argo profile observations[5]. Composited salinity anomaly profiles (Fig. 3d–f), constructed from ONI-classified El Niño and La Niña periods, show that during El Niño salinity is elevated throughout the entire upper water column from the surface to 400–600 m depth, and particularly the SSM strengthens by over 0.02 g kg^{-1} across all three subdomains. Within the STUW density layer, El Niño composites are 0.03–0.05 g kg^{-1} saltier than La Niña, with the strongest signal in the Eastern Caribbean (0.054 g kg^{-1}) (Supplementary Fig. 2a–c). The

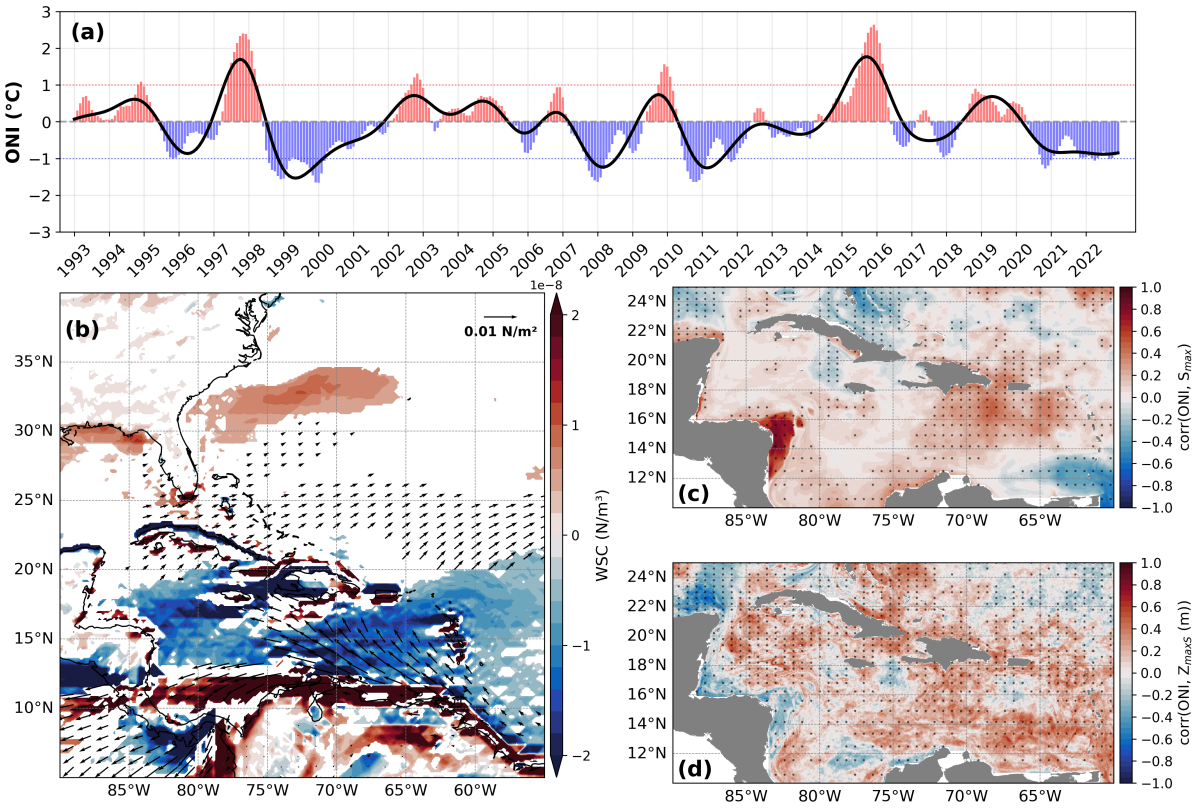

Fig. 2. ENSO forcing and spatial response of the Caribbean SSM. (**a**) Monthly (bars) and lowpass-filtered (black) Oceanic Niño Index (ONI) time series. (**b**) Wind stress and wind stress curl regressed on ONI. (**c**,**d**) Correlation maps of $S_{\max}$ and $Z_{\max S}$ with ONI.

Caribbean SSM (i.e., $Z_{\max S}$) deepens by ~5 m during El Niño and shoals by ~5 m during La Niña, creating a total $Z_{\max S}$ vertical displacement of ~10 m across ENSO cycles. The corresponding T–S diagrams (Fig. 3g–i) confirm that the saltier maximum salinity water is accompanied by the presence of STUW during El Niño, indicating a causal relationship between strengthened STUW inflow and the SSM.

Mechanisms linking ENSO and the SSM

ENSO exerts strong impacts on both the regional atmospheric circulation and oceanic advection driven by open-ocean forcing, which ultimately affect the subsurface salinity structure in the Caribbean. The interannual time series of ONI, regional wind stress curl, STUW salt transport, $S_{\max}$, and $Z_{\max S}$ reveal a coherent chain of high correlations linking Pacific climate variability to Caribbean subsurface salinity (Fig. 4; Table 1). The WSC over the Caribbean (12–20°N, 85–60°W) is significantly anticorrelated with ONI at zero lag ($r = -0.55$), demonstrating that El Niño (La Niña) events favor negative (positive) WSC anomalies (Fig. 4b), as also revealed by the regressed WSC pattern in Fig. 2b. The peak negative correlation occurs at lag −3 months ($r = -0.62$), indicating that the WSC response develops nearly

Table 1. Pearson correlation coefficients between low-pass filtered time series of the ONI, area-averaged WSC, STUW salt transport, maximum salinity ($S_{\max}$) anomalies, and $Z_{\max S}$ anomalies for Caribbean subdomains over 1993–2022. For each variable pair, the zero-lag correlation r_0 and/or maximum correlation with its lag $r_{\max}$ are shown. Positive lag indicates that the second variable lags the first.

	r_0 (corr, lag)	$r_{\max}$ (corr, lag)
r(ONI, WSC)	(−0.55, 0)	/
r(ONI, STUW)	(0.66, 0)	/
r(ONI, $S_{\max}$-Carib)	(0.34, 0)	(0.54, 10)
r(ONI, $S_{\max}$-East)	(0.33, 0)	(0.45, 9)
r(ONI, $S_{\max}$-Central)	(0.35, 0)	(0.54, 9)
r(ONI, $S_{\max}$-NW)	(0.28, 0)	(0.53, 12)
r(ONI, $Z_{\max S}$-Carib)	/	(−0.41, 22)
r(ONI, $Z_{\max S}$-East)	/	(−0.42, 21)
r(ONI, $Z_{\max S}$-Central)	/	(−0.39, 23)
r(ONI, $Z_{\max S}$-NW)	/	(−0.34, 24)
r(STUW, $S_{\max}$-Carib)	/	(0.59, 14)
r(STUW, $S_{\max}$-East)	/	(0.53, 9)
r(STUW, $S_{\max}$-Central)	/	(0.61, 13)
r(STUW, $S_{\max}$-NW)	/	(0.61, 18)
r(WSC, $Z_{\max S}$-Carib)	(−0.42, 0)	(−0.45, 3)
r(WSC, $Z_{\max S}$-East)	(−0.53, 0)	(−0.54, 2)
r(WSC, $Z_{\max S}$-Central)	(−0.51, 0)	(−0.53, 2)
r(WSC, $Z_{\max S}$-NW)	(−0.19, 0)	(−0.27, 7)

simultaneously with the ENSO peak.

A density-based STUW salt transport index confirms that changes in subtropical inflow of saline water accompany the local wind-driven adjustment (Fig. 4c). ONI and STUW salt transport are strongly positively correlated ($r = +0.66$ at zero lag). During El Niño, high-salinity STUW transport increases by ∼0.2–0.4 $\times 10^{11}$ g s^{-1}, enhancing the supply of saline water to the Caribbean. La Niña years show the reverse, with weakened inflow and lowered subsurface salinity (Fig. 4d).

The depth of the SSM ($Z_{\max S}$) shows a delayed negative correlation with ONI (Fig. 4e): the peak anticorrelations occur at lags of +21 to +24 months (Table 1). This indicates that following El Niño events, the $S_{\max}$ core becomes shallower with a delay of ∼20 months, substantially longer than the $S_{\max}$ amplitude response (∼10–12 months). The sign is physically consistent: El Niño enhances STUW salt transport and strengthens the SSM (i.e., $S_{\max}$), and the subsequent La Niña phase (which follows ∼12–18 months after El Niño) drives shoaling through anomalous positive WSC (Ekman suction). Notably, the WSC–$Z_{\max S}$ relationship is much more immediate and stronger than the ONI–$Z_{\max S}$ relationship, with peak correlations at lags of only +2 to +7 months ($r = -0.54$ to -0.53 for Eastern and Central; Table 1). This contrast suggests that $Z_{\max S}$ is primarily controlled by local wind-driven Ekman dynamics, while the $S_{\max}$ amplitude is more strongly influenced by remote advective processes through STUW salt transport.

Both WSC and STUW salt transport are significantly correlated with $S_{\max}$ across the Caribbean subdomains. The most striking feature is the consistent lag of +9 to +12 months between ONI and $S_{\max}$: the Eastern Caribbean peaks earliest (lag +9 months, $r = +0.45$); Central Caribbean at lag +9 months ($r = +0.54$); Northwest Caribbean latest at lag +12 months ($r = +0.53$); whole Caribbean at lag +10 months ($r = +0.54$). This westward-to-northwestward progression is consistent with advective propagation of the salinity signal carried by the CTF through the Caribbean basin (Fig. 1b). The ~10-month delay from the ENSO peak to the maximum salinity response reflects the cumulative time required for (1) wind-driven circulation changes to adjust STUW transport ($r(\mathrm{ONI}, \mathrm{STUW}) = -0.66$, lag ~0–3 months, nearly immediate); (2) advection of the salinity anomaly through the subtropical gyre into the Caribbean (~6–10 months); and (3) vertical and lateral mixing to modify the SSM (additional months).

These findings suggest two coupled mechanisms through which ENSO modulates Caribbean SSM magnitude and depth. First, **local control**: ENSO-related wind stress curl anomalies alter the vertical position of the salinity core ($Z_{\max S}$) through Ekman pumping/suction. During El Niño (La Niña), negative (positive) WSC anomalies induce anomalous downwelling (upwelling) that deepens (shoals) the SSM. Second, **remote control**: ENSO teleconnection, through large-scale air–sea interaction, affects the westward advection of STUW within the subtropical gyre. Enhanced (weakened) STUW transport during El Niño (La Niña) conveys more (less) high-salinity water into the Caribbean through the passages in the east.

Discussion

This study highlights how ENSO as the primary driver modulates the interannual variability of subsurface salinity in the Caribbean Sea. Using 30 years of high-resolution, data-assimilative ocean reanalysis data, we have found that the Subsurface Salinity Maximum (SSM) and its depth are not just random fluctuations, but rather closely related to the large-scale air–sea interactions originating in the Pacific. Essentially, El Niño events set the stage for a saltier and deeper SSM, while La Niña phases correspond with fresher, shallower layers. During El Niño, we observed salinity increases of approximately 0.02 g kg^{-1} across the upper water column and even stronger anomalies within the Subtropical Underwater (STUW), which can be 0.03 to 0.05 g kg^{-1} saltier than La Niña averages. In the whole Caribbean, this saltier SSM is always accompanied by a deepening of about 10 meters during El Niño.

The mechanism behind this regime shift is two-fold, involving both local atmospheric changes and remote oceanic transport. First, ENSO-related wind stress curl (WSC) anomalies directly impact the

vertical position of the salinity core through Ekman pumping/suction. During El Niño (La Niña), negative (positive) WSC anomalies trigger anomalous downwelling (upwelling) that physically pushes the high-salinity core deeper (shallower). Second, the STUW forms in the North Atlantic Subtropical Gyre through a combination of Ekman pumping and lateral induction at the base of the winter mixed layer[19]. Its interannual subduction rate variability is governed primarily by winter mixed layer depth changes driven by the concurrent effects of the NAO and ENSO teleconnections. Once subducted, the STUW spreads as a westward-propagating salinity maximum along the $\sigma_\theta \approx 25.5$ kg m^{-3} isopycnal surface within the subtropical gyre; however, Qu et al.[19] were unable to track this propagation west of approximately 50°W due to sparse Argo data coverage, leaving the STUW pathways into the Caribbean Sea and the linkage between formation and downstream salinity anomalies an open question. Our study addresses this gap directly: we show that during El Niño (La Niña), this westward salt transport carried by STUW is enhanced (weakened), delivering additional high-salinity water through the Windward Island and Leeward Island Passages and into the Caribbean basin, ultimately changing the SSM propagation along the CTF. These dynamics emphasize the Caribbean's role as a vital "sensitive node" in the global climate system, where Pacific variability leaves a distinct footprint on Atlantic thermohaline properties.

While these findings provide a clearer picture of the Pacific–Atlantic connection, we acknowledge certain model-specific constraints that frame the scope of this work. The inherent sensitivity to vertical mixing within the water column, a common characteristic in data-assimilative reanalysis, may slightly smooth the salinity gradients, yet the strength of the interannual signal remains statistically significant. Furthermore, while the current ocean-only model was selected to isolate the oceanic response to external forcing, we recognize that the absence of a fully coupled air–sea module means that local feedback loops could be further refined in future iterations. We also view the influence of mesoscale features, such as eddy activities, as a critical "next step" for future research, as these features likely contribute to the water mass transformation while propagating westward. Despite these limitations, understanding this link is crucial for predicting how the Caribbean will modulate upper-ocean buoyancy and potentially influence the North Atlantic ocean circulation and regional climate under future climate scenarios. Moving forward, continued monitoring and refined modeling of this connection will be essential for anticipating how these signals evolve in a changing climate.

Methods

Model configuration

We use simulations from the Coupled Northwest Atlantic Prediction System version 2 (CNAPS2), a data-assimilative regional ocean model based on the Regional Ocean Modeling System (ROMS)[20]. The model domain spans the northwestern Atlantic (5–50°N, 100–55°W) and resolves mesoscale features with a resolution of up to 4 km horizontally and 50 sigma levels vertically. CNAPS2 assimilates satellite-altimetry-derived sea level anomalies, sea surface temperature, and T/S profiles from Argo floats and gliders using an Ensemble Optimal Interpolation (EnOI) data assimilation scheme, producing dynamically consistent analyses from January 1993 to December 2022. The model output includes daily-averaged salinity, temperature, velocity, and sea surface height. For this study, we calculate monthly averages of these variables and extract the maximum salinity ($S_{\max}$) and its corresponding depth ($Z_{\max S}$) at each grid point within the Caribbean Sea (10–25°N, 90–60°W).

Climate indices and statistical analysis

ENSO variability is characterized using the Oceanic Niño Index (ONI) obtained from NOAA's Climate Prediction Center, defined as the 3-month running mean of SST anomalies in the Niño-3.4 region (5°N–5°S, 120–170°W). Positive and negative ONI phases correspond to El Niño and La Niña events, respectively. To isolate signals within the ENSO frequency range, we apply either a 24-month low-pass filter or a 2–7 year band-pass filter to remove higher-frequency noise from the time series. We employ correlation analyses between various factors and the model-derived $S_{\max}$ and $Z_{\max S}$ fields to quantify ENSO's influence on them. Composite analyses and regression maps are used to identify ENSO-related forcing and oceanic response. Composite analyses are conducted for El Niño and La Niña periods with ONI thresholds over ±0.5°C (El Niño ≥ +0.5°C or La Niña ≤ −0.5°C).

Atmospheric and oceanic forcing

To examine the broader impacts of atmospheric forcing, we analyze wind and wind stress curl (WSC) anomalies derived from the ERA5 reanalysis, which is also used as forcing for CNAPS2. Wind stress and wind stress curl are computed as follows:

$$\boldsymbol{\tau} = \rho_a \, C_D \, |\mathbf{U}_{10}| \, \mathbf{U}_{10}, \tag{1}$$

$$\nabla \times \boldsymbol{\tau} = \frac{\partial \tau_y}{\partial x} - \frac{\partial \tau_x}{\partial y}, \tag{2}$$

where $\boldsymbol{\tau}$ is the wind stress vector (N m^{-2}), ρ_a is air density, C_D is the drag coefficient, and $\mathbf{U}_{10}$ is the wind velocity (m s^{-1}) at 10 m above sea surface. τ_x and τ_y are zonal (west–east) and meridional (north–south) wind components in x and y directions, respectively. WSC has units of N m^{-3}.

We examine SSM spatial variability by segmenting the Caribbean Sea into Northwest (NW), Central, and Eastern subdomains (Fig. 1a). We further evaluate the vertical salinity–temperature structure through vertical profiles and T–S diagrams for the whole Caribbean and these three subdomains. The connection with STUW formation and transport is examined using a density-based water mass tracer ($\sigma \approx 24.5$–26.0 kg m^{-3};[19]) to quantify inflow strength through the 69°W section (Fig. 1a) and its modulation by ENSO. The STUW salt transport is computed as:

$$S_{\mathrm{STUW}} = \rho_0 \int_{y_0}^{y_1} \int_{\sigma_{\mathrm{lower}}}^{\sigma_{\mathrm{upper}}} u(y,\sigma) \cdot S(y,\sigma)\, dy\, d\sigma, \tag{3}$$

where ρ_0 is the reference seawater density (1025 kg m^{-3}), and $u(y,\sigma)$ and $S(y,\sigma)$ are zonal velocity and salinity at each grid point in the meridional section between two density layers σ_{lower} and σ_{upper}. The STUW salt transport has units of g s^{-1}.

Data availability

The Oceanic Niño Index (ONI) data used in this study are provided by the NOAA Climate Prediction Center and are available at https://www.cpc.ncep.noaa.gov/products/analysis_monitoring/ensostuff/ONI_v5.php. ERA5 reanalysis data were retrieved from the Copernicus Climate Data Store at https://cds.climate.copernicus.eu/datasets/reanalysis-era5-single-levels. CNAPS2 ocean reanalysis output that supports the findings of this study is available from the corresponding author upon reasonable request.

Code availability

Analysis scripts used to generate the figures and statistics in this study will be made available via version-control repository upon acceptance for publication. The Regional Ocean Modeling System (ROMS) is open-source software available at https://www.myroms.org.

References

[1] Arnold L. Gordon. Circulation of the Caribbean Sea. *Journal of Geophysical Research (1896-1977)*, 72(24):6207–6223, 1967. ISSN 2156-2202. doi: 10.1029/JZ072i024p06207. URL https://onlinelibrary.wiley.com/doi/abs/10.1029/JZ072i024p06207. _eprint: https://agupubs.onlinelibrary.wiley.com/doi/pdf/10.1029/JZ072i024p06207.

[2] William J. Schmitz and Philip L. Richardson. On the sources of the Florida Current. *Deep Sea Research Part A. Oceanographic Research Papers*, 38:S379–S409, January 1991. ISSN 0198-0149. doi: 10.1016/S0198-0149(12)80018-5. URL https://www.sciencedirect.com/science/article/pii/S0198014912800185.

[3] W.Douglas Wilson and William E. Johns. Velocity structure and transport in the Windward Islands Passages. *Deep Sea Research Part I: Oceanographic Research Papers*, 44(3):487–520, March 1997. ISSN 0967-0637. doi: 10.1016/S0967-0637(96)00113-6. URL https://www.sciencedirect.com/science/article/pii/S0967063796001136.

[4] Matthew W. Schmidt, Howard J. Spero, and David W. Lea. Links between salinity variation in the Caribbean and North Atlantic thermohaline circulation. *Nature*, 428(6979):160–163, March 2004. ISSN 1476-4687. doi: 10.1038/nature02346. URL https://www.nature.com/articles/nature02346. Publisher: Nature Publishing Group.

[5] Joseph C. Gradone, T. N. Miles, J. B. Palter, S. M. Glenn, and W. D. Wilson. Warming and salinity changes of the upper ocean Caribbean through-flow since 1960. *Scientific Reports*, 15(1):23157, July 2025. ISSN 2045-2322. doi: 10.1038/s41598-025-05494-z. URL https://www.nature.com/articles/s41598-025-05494-z. Publisher: Nature Publishing Group.

[6] Rafael Ricardo Torres, Sadid Latandret, Jhon Salon, and Claudia Dagua. Water masses in the Caribbean Sea and sub-annual variability in the Guajira upwelling region. *Ocean Dynamics*, 73 (2):39–57, February 2023. ISSN 1616-7228. doi: 10.1007/s10236-022-01529-5. URL https://doi.org/10.1007/s10236-022-01529-5.

[7] Joseph C. Gradone, W. Douglas Wilson, Scott M. Glenn, and Travis N. Miles. Westward modification of caribbean through-flow water mass structure. *Deep Sea Research Part I: Oceanographic Research Papers*, 225:104581, 2025. ISSN 0967-0637. doi: https://doi.org/10.

1016/j.dsr.2025.104581. URL https://www.sciencedirect.com/science/article/pii/S0967063725001396.

[8] Ruth Curry, Bob Dickson, and Igor Yashayaev. A change in the freshwater balance of the atlantic ocean over the past four decades. *Nature*, 426(6968):826–829, Dec 2003. ISSN 1476-4687. doi: 10.1038/nature02206. URL https://doi.org/10.1038/nature02206.

[9] Hao Liu, Lisan Yu, and Xiaopei Lin. Recent decadal change in the north atlantic subtropical underwater associated with the poleward expansion of the surface salinity maximum. *Journal of Geophysical Research: Oceans*, 124(7):4433–4448, 2019. doi: https://doi.org/10.1029/2018JC014508. URL https://agupubs.onlinelibrary.wiley.com/doi/abs/10.1029/2018JC014508.

[10] Hui-Jun Wang, Ren-He Zhang, Julie Cole, and Francisco Chavez. El Niño and the related phenomenon Southern Oscillation (ENSO): The largest signal in interannual climate variation. *Proceedings of the National Academy of Sciences*, 96(20):11071–11072, September 1999. doi: 10.1073/pnas.96.20.11071. URL https://www.pnas.org/doi/10.1073/pnas.96.20.11071.

[11] Chunzai Wang. Variability of the Caribbean Low-Level Jet and its relations to climate. *Climate Dynamics*, 29(4):411–422, September 2007. ISSN 1432-0894. doi: 10.1007/s00382-007-0243-z. URL https://doi.org/10.1007/s00382-007-0243-z.

[12] Y.-L. Chang and L.-Y. Oey. Coupled Response of the Trade Wind, SST Gradient, and SST in the Caribbean Sea, and the Potential Impact on Loop Current's Interannual Variability. *Journal of Physical Oceanography*, July 2013. doi: 10.1175/JPO-D-12-0183.1. URL https://journals.ametsoc.org/view/journals/phoc/43/7/jpo-d-12-0183.1.xml.

[13] Aida Alvera-Azcárate, Alexander Barth, and Robert H. Weisberg. The Surface Circulation of the Caribbean Sea and the Gulf of Mexico as Inferred from Satellite Altimetry. *Journal of Physical Oceanography*, March 2009. doi: 10.1175/2008JPO3765.1. URL https://journals.ametsoc.org/view/journals/phoc/39/3/2008jpo3765.1.xml.

[14] Minghai Huang, Xinfeng Liang, Yang Yang, and Yang Zhang. ENSO Modulates Mean Currents and Mesoscale Eddies in the Caribbean Sea. *Geophysical Research Letters*, 50 (15):e2023GL103958, August 2023. ISSN 1944-8007. doi: 10.1029/2023GL103958. URL https://onlinelibrary.wiley.com/doi/abs/10.1029/2023GL103958. _eprint: https://onlinelibrary.wiley.com/doi/pdf/10.1029/2023GL103958.

[15] Margarita E. López-Álzate, Juan-Manuel Sayol, Ismael Hernández-Carrasco, Andrés F. Osorio, Evan Mason, and Alejandro Orfila. Mesoscale eddy variability in the Caribbean Sea. *Ocean Dynamics*, 72(9-10):679–693, September 2022. ISSN 1616-7228. doi: 10.1007/s10236-022-01525-9. URL https://doi.org/10.1007/s10236-022-01525-9.

[16] L. M. Chérubin and P. L. Richardson. Caribbean current variability and the influence of the Amazon and Orinoco freshwater plumes. *Deep Sea Research Part I: Oceanographic Research Papers*, 54(9):1451–1473, September 2007. ISSN 0967-0637. doi: 10.1016/j.dsr.2007.04.021. URL https://www.sciencedirect.com/science/article/pii/S0967063707001082.

[17] Victoria J. Coles, Maureen T. Brooks, Julia Hopkins, Michael R. Stukel, Patricia L. Yager, and Raleigh R. Hood. The pathways and properties of the Amazon River Plume in the tropical North Atlantic Ocean. *Journal of Geophysical Research: Oceans*, 118(12):6894–6913, December 2013. doi: 10.1002/2013JC008981. URL https://agupubs.onlinelibrary.wiley.com/doi/10.1002/2013JC008981.

[18] Giovanni Seijo-Ellis, Donata Giglio, Gustavo Marques, and Frank Bryan. CARIB12: a regional Community Earth System Model/Modular Ocean Model 6 configuration of the Caribbean Sea. *Geoscientific Model Development*, 17(24):8989–9021, December 2024. ISSN 1991-959X. doi: 10.5194/gmd-17-8989-2024. URL https://gmd.copernicus.org/articles/17/8989/2024/.

[19] Tangdong Qu, Linlin Zhang, and Niklas Schneider. North Atlantic Subtropical Underwater and Its Year-to-Year Variability in Annual Subduction Rate during the Argo Period. *Journal of Physical Oceanography*, 46(6):1901–1916, June 2016. doi: 10.1175/JPO-D-15-0246.1. URL https://journals.ametsoc.org/view/journals/phoc/46/6/jpo-d-15-0246.1.xml.

[20] Ruoying He, Tianning Wu, Shun Mao, Haibo Zong, Joseph Zambon, Jennifer Warrillow, Jennifer Dorton, and Debra Hernandez. Advanced Ocean Reanalysis of the Northwestern Atlantic: 1993-2022, March 2025. URL http://arxiv.org/abs/2503.06907. arXiv:2503.06907 [physics].

Acknowledgements

This research was supported by the National Science Foundation (NSF) under grants RISE-2019758, OCE-2206052, OCE-2421623, OCE-2421624, CNS-2223844, and OAC-2417850. Additional support

from the National Academies of Sciences, Engineering, and Medicine (NASEM) Gulf Research Program is gratefully acknowledged.

Author contributions

Y.D. designed the study, performed the analyses, and drafted the manuscript. T.W. assisted with software and statistical analysis. J.C.G. and T.N.M. contributed to interpretation of subsurface salinity observations and provided Argo-based context. W.D.W. contributed to interpretation of regional circulation and water mass pathways. R.H. supervised the project, developed the modeling framework, and edited the manuscript. All authors discussed the results and contributed to the final manuscript.

Competing interests

The authors declare no competing interests.

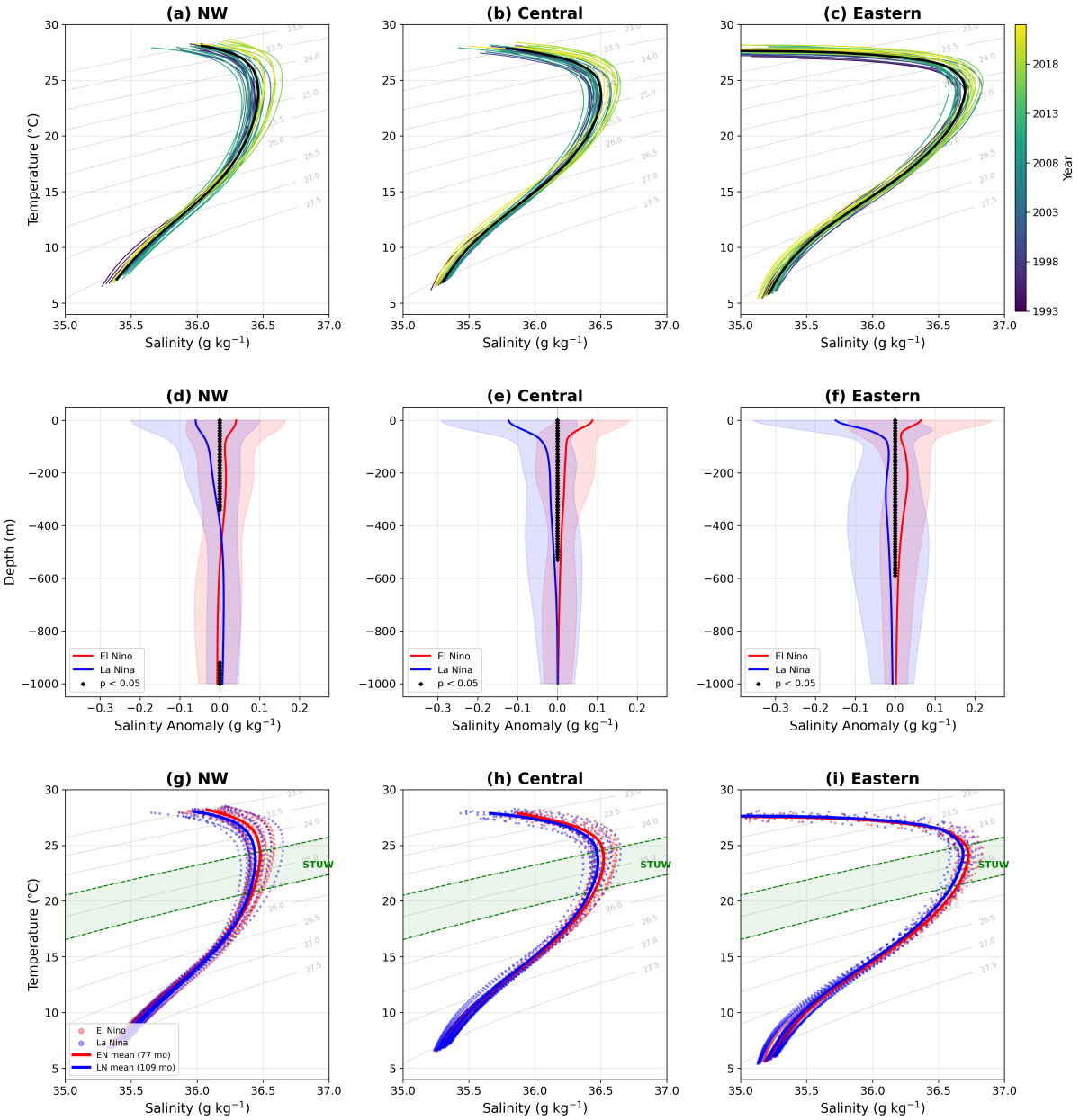

Fig. 3. ENSO composites of the Caribbean SSM vertical structure. Vertical profiles and T–S diagrams showing ENSO composites of the SSM layer for NW, Central, and Eastern Caribbean. (**a–c**) Interannual T–S profiles (1993–2022, color-coded by year). (**d–f**) ENSO-composited salinity anomaly profiles (El Niño vs. La Niña, with black dots showing depths passing the 95% confidence *t* test). (**g–i**) ENSO-composited T–S diagrams with STUW water type highlighted.

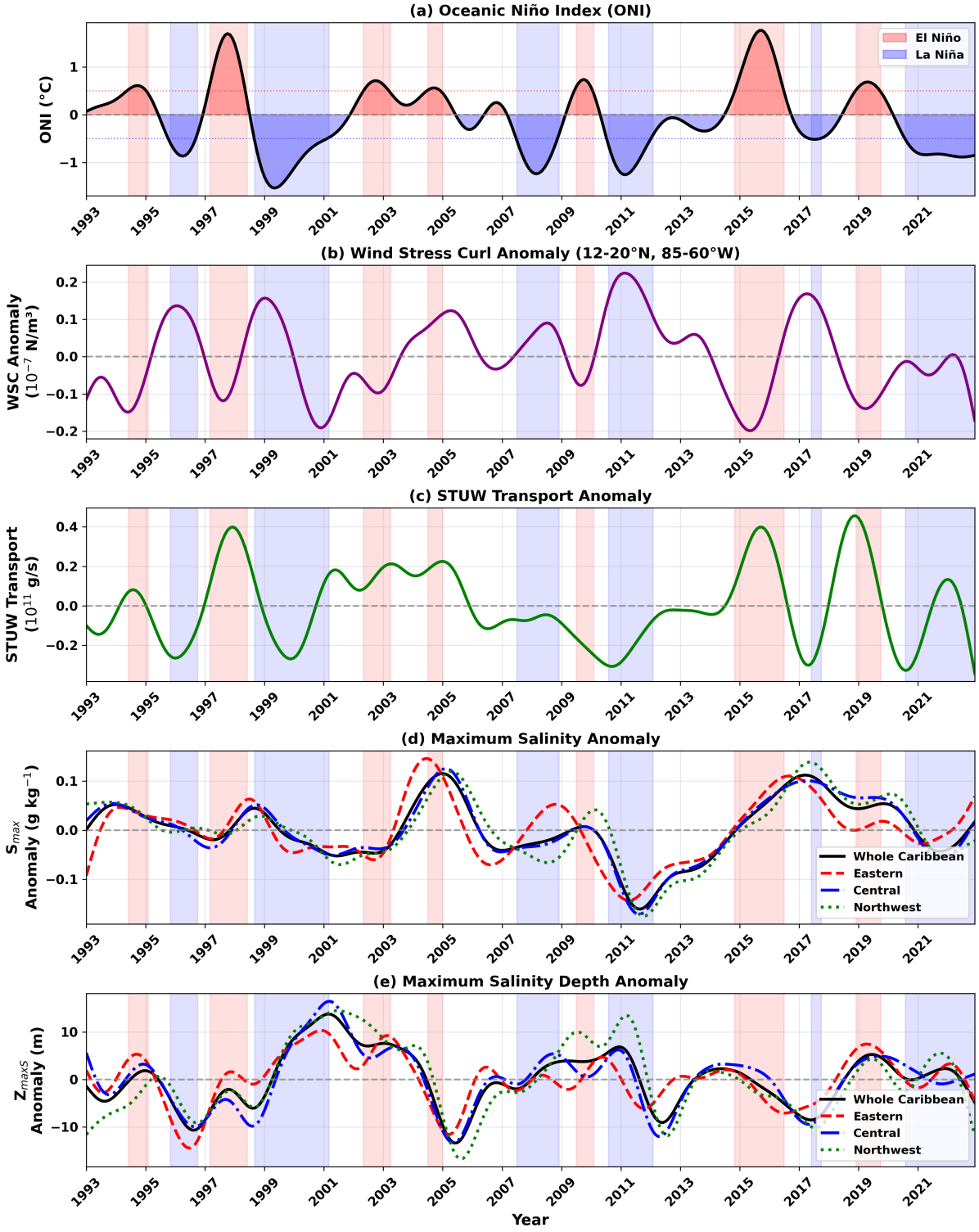

Fig. 4. Coherent time-series response of the Caribbean SSM to ENSO. Time series of ONI, wind stress curl (WSC), STUW salt transport, $S_{\max}$, and $Z_{\max S}$ anomalies over the period 1993–2022.

Supplementary Information for: ENSO-Driven Modulation of the Caribbean Subsurface Salinity Maximum

Yongfei Deng, Tianning Wu, Joseph C. Gradone, W. Douglas Wilson,
Travis N. Miles, and Ruoying He*

*Corresponding author: rhe@ncsu.edu

Contents

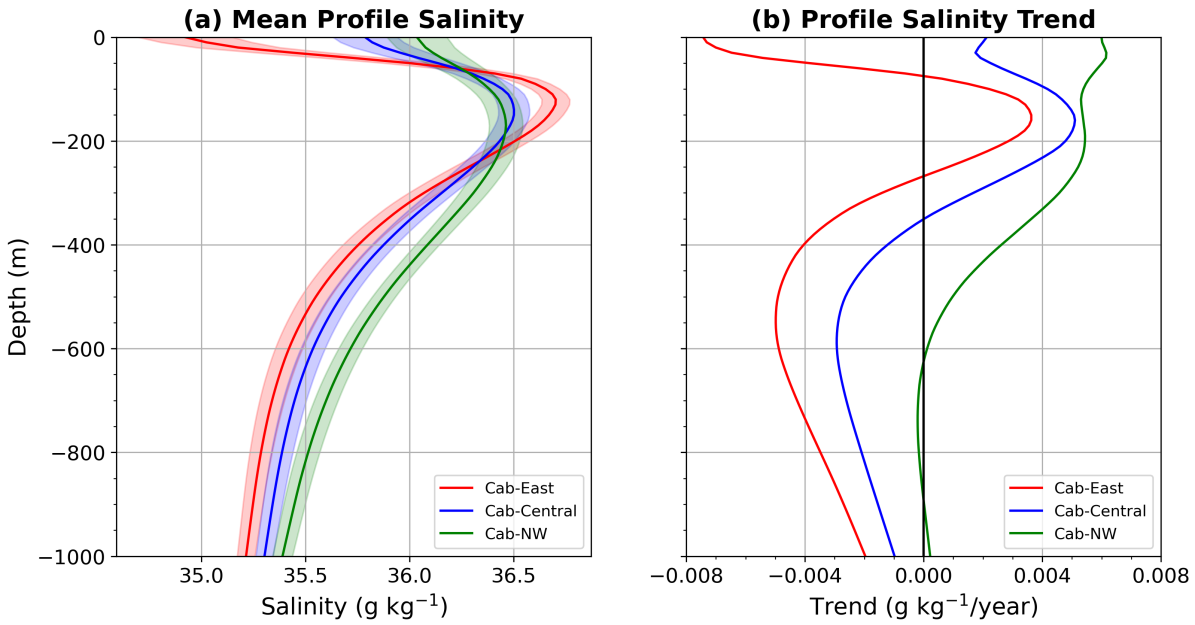

Supplementary Fig. S1. Mean and trend of upper 1000 m salinity profiles in Eastern, Central, and NW Caribbean.

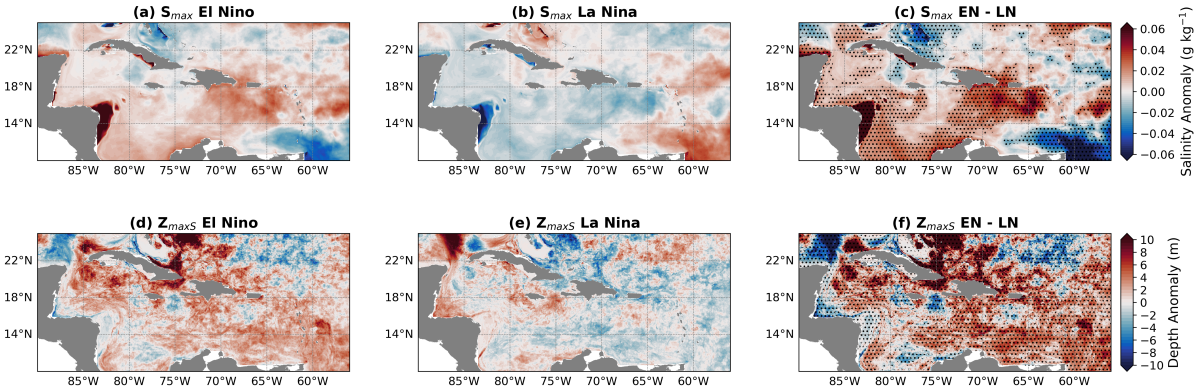

Supplementary Fig. S2. ENSO composites of the Caribbean SSM. ENSO-composited $S_{\max}$ and $Z_{\max S}$ and differences between El Niño and La Niña events.